Reynolds Averaged Navier-Stokes Analysis for Civil Transport Aircraft using Structured and Unstructured grids

Vishal S. Shirbhate
CTFD Division, National Aerospace Laboratories, CSIR, Bangalore

Abstract

The current study deals with the two different mesh generation strategies demonstrated for the RANS simulations over a typical civil transport aircraft near transonic regime. The commercial grid generator ICEM-CFD is used for meshing and High Resolution Flow Solver on Unstructured Meshes (HiFUN)[Ref.1] is used as a solver for the numerical computations. The accurate prediction of aerodynamic coefficients is an important design parameter in preliminary design phase of civil transport aircraft. The hybrid tetrahedral & prismatic unstructured mesh and mapped hexahedral mesh are generated. In the absence of experimental results, the simulated results are compared with the CFD (RANS) data available from Computational Research Laboratories (CRL)[Ref.2] , Pune.

It is reported in the literature that any grid used for computing in such flow regime should not only be fine near the body but also in the region sufficiently away from the body in order to capture the shock strength precisely. An attempt has been made to satisfy the aforementioned criteria by placing a far-field boundary condition sufficiently away (typically about hundreds chords) from the body. The results presented in the paper thoroughly demonstrate the unstructured grid methodology developed with minimal number of cells that matches reasonably well between twice the number of in-housed generated mapped hexahedral cells and CRL unstructured mesh.

Key-words : Navier-Stokes Analysis, Unstructured Grid, Structured Grid, Civil Transport Aircraft, aerodynamic coefficients

Nomenclature

C_L	=	Lift Co-efficient
C_D	=	Drag Co-efficient
C_M	=	Pitching Moment Co-efficient
c	=	chord
Re. No.	=	Reynolds Number
M.No.	=	Mach Number
Pax.	=	Number of Passengers

**Scientist, CTFD Division, CSIR-NAL, Post Box No.1779, Bangalore-560017, e-mail: vishalss@nal.res.in*

1.Introduction

In the preliminary design phase (PDP) of transport aircraft , the configuration of the aircraft changes regularly to meet the design criteria of various disciplines. The wind tunnel experiments for every configurations is not considered as a feasible option at such initial stage. Hence the CFD plays a very important role as a design tool in PDP of aircraft design [Ref.3]. The aircraft designer often looks for a aerodynamic loads generated, especially C_L and C_D in quick time frame from CFD computations to check whether there is a need to change the design or not. This requires accurate prediction of flows over the aircraft configurations.

The aim of the current work is to establish a complete RANS CFD facility within a design bureau that helps in generating a aerodynamic loads in quick time for future aircraft configurations. The present paper also details the two different grid generation approaches and specific techniques used. The current civil transport aircraft comprises of fuselage, wing, horizontal and vertical tail. It does not carry any engine-nacelle attachment. The wing-fuselage-fairing area is considered as a critical region during mesh generation process and hence, fairly well captured in both types of grids. The Drag Prediction Workshop (DPW) [Ref.4] guidelines have been followed for the entire mesh generation process. It is also reported in the literature that the structured mesh produces good CFD results because of its most often flow-aligned nature. These types of grids utilize quadrilateral elements in 2D and hexahedral elements in 3D in a computationally rectangular array. The major drawback of structured block grids is the time and expertise required to lay out an optimal block structure for an entire model. Often this comes down to past user experience and brute force placement of control points and edges. Some geometries, eg. shallow cones and wedges, do not lend themselves to structured block topologies. In these areas, the user is forced to stretch or twist the elements to a degree which drastically affects solver accuracy and performance.Unstructured grid methods utilize an arbitrary collection of elements to fill the domain.. These types of grids typically utilize triangles in 2D and tetrahedral in 3D. The advantage of unstructured grid methods is that they are very automated and, therefore, requires less effort.

In, the present work, numerical experiments are performed on structured and unstructured mesh for 90 passenger variant which predicts satisfactorily results. Also, it is shown that a carefully generated minimal number of unstructured grid can predict results comparable to the corresponding structured grid.

2. Mesh Generation and Solver Settings

This section details grid generation strategy used in generating both 'mapped hexahedral' and 'tetrahedral-prism meshes' in ICEM-CFD environment [Ref.5].

2.a Tetrahedral Mesh :

These types of grids utilize triangles in 2D and tetrahedral cells in 3D. The user need not worry about laying out block structure or connections. Unstructured methods also enable the solution of very large and detailed problems in a relatively short period of time. The major drawback of unstructured grids is the lack of user control when laying out the mesh. But it can be overcome by proper setting of initial parameters and growth ratio. The major advantage of this type of grid method is that they are fully automated and, therefore, require less user time. The Fig.1 shows the surface mesh over the aircraft.

The methodologies adopted for the unstructured mesh generation are mentioned below:

- Volume domain has typical hemi-spherical shape and comprises of 100 chord length
- The first grid cell distance applied within a boundary layer is 5 micron for a y+ [Ref.6] equals to 1 and growth ratio of 1.2 is adopted to the viscous layers. The growth factor of 1.2 is considered for the tetrahedral cells for the proper laying out of the mesh. It also helps to properly capture the vortices generated.
- The aspect ratio and element quality (quality check > 0.3) for the generated mesh is within the acceptable limit.
- Wing surface is divided near leading and training edge along the span to capture the suction peak and separation accurately as shown in Fig. 2. The same methodology is used for HT and VT.

**Scientist, CTFD Division, CSIR-NAL, Post Box No.1779, Bangalore-560017, e-mail: vishalss@nal.res.in*

- Equilateral triangle elements are generated in TE of wing ,HT and VT to capture proper TE effects which is seen in Fig.3
- Wing-Fuselage-Fairing junction[Ref.7] has been meshed very fined enough to capture separation and shocks as shown in Fig.4.
- It is to be noted that Icem-CFD feature 'density' is used around the aircraft geometry to ensure fine mesh generation around the aircraft surface.
- No. of Boundary Layers= 30 with 1st two layers of constant spacing as shown in Fig.5 (as per DPW guidelines)
- Total Mesh Size = 27 million

4.b Hexahedral Mesh :

The volume domain of hexahedral mesh is shown in Fig.6. It also represents the overall block strategy applied for the mesh generation. The Fig.7 shows the surface mesh over the aircraft. Figure 8 & 9 shows Mesh near wing-winglet junction and at the wing crank location respectively.

Features:

- Volume domain is a parabolic C-shape and is considered because of its convenience of implementation in HiFUN and other commercial CFD solvers
- Upstream distance = 80 c, downstream distance = 100 c, spanwise distance = 80 c, Top and Bottom distance = 80 c each
- First grid cell distance in boundary layer =5 micron for y+ equals to 1
- Growth ratio =1.25 max
- Elements quality = 0.28 (quality check)
  = 0.42 (determinant 3x3x3 check)
- The element size at wing L.E. is kept 0.1% of winglet tip chord and T.E. is 0.1% of wing root chord to capture suction peak and separation accurately. Similar methodology has been employed at HT and VT.
- Total number of blocks = 400
- Total Mesh size = 48 million

Geometry Parameters	Details
Span, b	270 units
Planform Area, S_{ref}	690 units
MAC	27 units
Moment Ref. point	160, 0, 0 units

Table.1. Geometry Parameters

3. Sign Convention:

The following sign convention is adopted for the current study

X Axis	+ve- towards aircraft tail
Y Axis	+ve - towards starboard side
Z Axis	+ve - upwards
Pitching Moment (CM)	+ve- nose upwards

Table.2. Sign Convention

4. Solver

The solver used for the present study is HiFUN which is a finite volume method based code. The solver is fine tuned to solve typical aerospace applications. HiFUN employs unstructured face based data. This makes the solver capable of handling grids with hexahedral, tetrahedral, prismatic, pyramidal or any combination of these basic mesh elements. HiFUN supports a number of numerical flux formulae for inviscid flux computation. For the present study, HLLC scheme is employed for computation of inviscid flux. The Spallart- Allmaras turbulence model is used for current steady-state computations. The HiFUN solver has been extensively used for solving a number of problems over a wide range of Mach No. The CFL number is varied linearly with the iteration number. The implementation of CFL number is based on the basis of pre-stall and post-stall regime. Aggressive CFL ramping (difference in CFL no. between two successive iterations) is used in pre-stall regime whereas slow ramping is imposed in post-stall regime to get a stable convergence in residuals.

The CRL has used commercial code CFD++ [Ref.8] (Metacomp Technologies) for the computations and Hypermesh grid generator for creating a unstructured mesh. The density based solver of CFD++ has been used for present study. CFD++ also employed a Spallart- Allmaras turbulence model for current steady-state computations.

Hardware Details:

All computations are performed on SGI Altix ICE 8400 EX Supercomputer facility situated at NAL-CMMACS [Ref.9]. The jobs are submitted using PBS batch mode. 264 processors are used for running a single job.

The flow conditions used for the computations are tabulated below:

Parameters	*Values*
Mach No	0.7
Reynolds No	15 million
Altitude (feet)	35000
Pressure (Pa)	23840.7
Temperature (K)	218.81
Dynamic Viscosity (Nsm-2)	1.43e-05

Table.3 Flow Conditions

5. Results

The present section represents the detail comparison of results for three different grids. As there is no experimental data available for present aircraft configuration, the in-housed generated grid results are compared with available CFD data from CRL. Fig.10 to Fig.13 depicts comparison of Cp [Ref.10] distribution at various span location for 0° angle of attack. The in-housed 'TET' mesh has 27 million cells compared to 48 million cells in-housed hexahedral and 60 million CRL unstructured mesh. The suction peak computed by in-housed 'TET' (tetrahedral-prism) grid are in good agreement with "HEX" (hexahedral) and available unstructured grid CFD results. The in-housed TET grid is fine enough on aircraft surface to capture peak pressures. Hence, even though it has less no. of grid cells , it shows close match with other two grid results.

Fig. 14 to Fig. 17 represents the Cp distribution at AoA= 4°. At this angle of attack, smeared shock is captured by all three grids. Also, it is seen that HEX and CRL results are in better agreement compared to in-housed TET grid. But the difference observed is very less. The detail investigation study is in progress to find the reason behind this occurrence. The first cut reason may be the coarseness of grid in volume domain.

The Fig.18 depicts C_L [Ref.11] curve v/s AoA. It shows a good match for a lift-curve slope in the linear region for all the three cases. CRL predicts higher C_{Lmax} compared to other two grids and predicts 11.5 counts higher C_{Lmax} compared to 'TET' and 21.3 counts higher C_{Lmax} compared to 'HEX' (1 count = 10-3 for C_L). However, the stall angle predicted for all grids are same. It shows that in-housed generated TET mesh is capable

to predict proper stall angle. The drag polar in Fig.19 shows that drag co-efficient predicted by three different grids are in close match with each other. But, the detail investigation shows in-housed generated TET grid slightly over-predicts drag.

Fig.20 shows pitching moment plot with lift co-efficient for all three grids. The negative slope for positive angle of attack indicates stability in pitching. The same trend has been captured by TET results along with other two grids.

Conclusion

The Navier-Stokes computations are carried out on NCA configuration for three different grids. The results generated by in-housed unstructured grid which has lowest mesh size shows good match with other grids. The in-housed unstructured grid is generated by giving more concentration on acceleration and separation region. The fine mesh distribution has been given at the regions of wing-body-fairing and wing-winglet region which results in very good match for C_P comparison at various cross sections along span. The C_{Lmax} prediction by in-housed TET grid at given flow condition are in better agreement with other two grids. However, slight modification is needed in in-housed TET mesh generation to further improve the leading edge region to capture the suction peak more accurately. From the overall study done, it can be concluded that the special in-housed methodologies developed for generation of unstructured grid has proven their maturity and are in better agreement with other two grids. It has least no of mesh size that consume less computational time hence improve the overall simulation efficiency time.

Acknowledgements:

The authors wish to thank Mr. H.N.Vijay, Head, Layout Team, NCAD, CSIR-NAL and Mr. R.Karthik, Sr. Design Engineer, NCAD for providing clean and smooth CAD models, which reduces geometry clean-up time. Also thanks to Mr. R. Thangavelu, Group Co-ordinator, HPC Group, CSIR-CMMACS and Dr. V.Y. Mudkavi, HOD, CTFD,CSIR-NAL for creating sufficient nodes at CMMACS-HPC facility on priority for the computations. Thanks are due to Mr. Abhishek Burman, Scientist-ADA for his guidance and technical support. Author also wish to thank Mr. Sonil Singh, Design Engineer, NCAD, for providing structured mesh. Special thanks to Asso. Prof.N. Balakrishnan, Aero. Dept., IISc, Dr. Nikhil Shende and Mr. Ravindra from SandI Team whose enormous support helped in mesh generation and in HiFUN solver setting process.

References:

[1] http://www.sandi.co.in
[2] P-CFD-NAL-CRL-NCA90-I Report , 01-08-2011
[3] Vos, J.B., Rizzi, A., Darracq, D., Hirschel, E.H., *Navier–Stokes solvers in European aircraft design*, Progress in Aerospace Sciences 38 (2002) 601–697
[4] http://aaac.larc.nasa.gov/tsab/cfdlarc/aiaa-dpw/Workshop4/workshop4.html
[5] ICEM-CFD user manual
[6] http://geolab.larc.nasa.gov/APPS/YPlus/
[7] Mathur, J.S., Dhanalakshmi, K., Ramesh, V. and Chakrabarty, S. K., *Aerodynamic design and analysis of SARAS aircraft, Computational Fluid Dynamics Journal,* Vol.16, No.3, pp.320-334,2008
[8] http://www.metacomptech.com/
[9] http://www.cmmacs.ernet.in/cmmacs/Computing/altix_ice_8400.html
[10] O, Akio., S, Eiji., A Drag Prediction Validation Study for Aircraft Aerodynamic Analysis
[11] Mathur, J.S., Dhanalakshmi, K.,and Chakrabarty, S. K., *Application of Advanced CFD Codes for Design and Development of SARAS Aircraft,* J. Aero. Sci. Technol., 2003, 55(3), 174-85

**Scientist, CTFD Division, CSIR-NAL, Post Box No.1779, Bangalore-560017, e-mail: vishalss@nal.res.in*

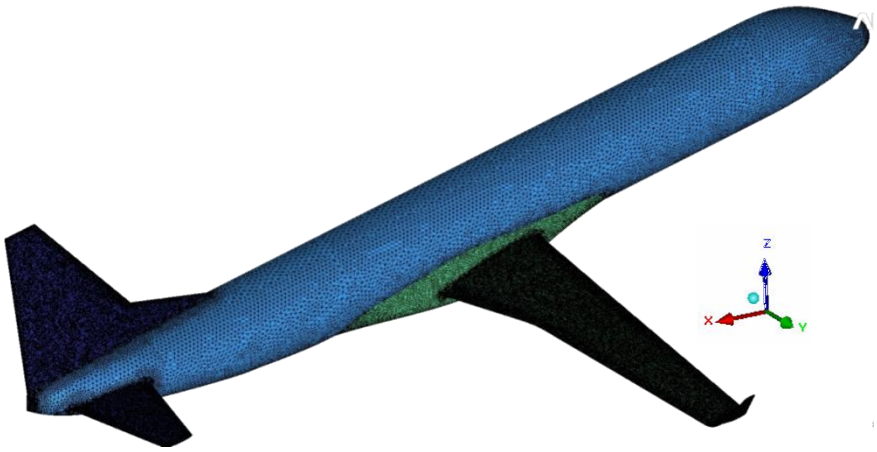

Fig.1 Unstructured Mesh over Aircraft

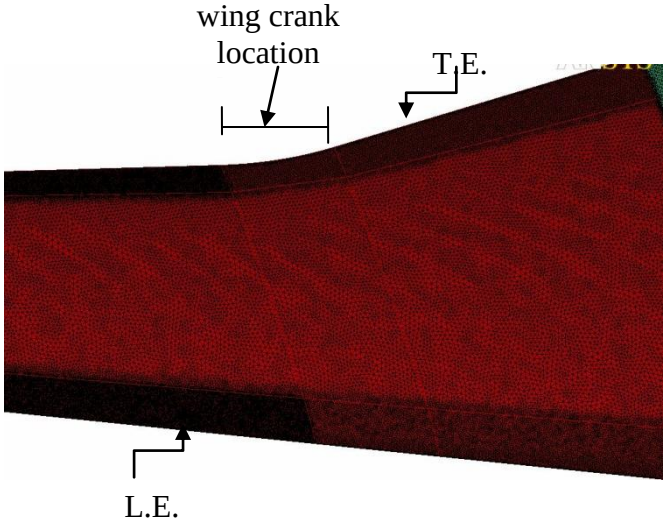

Fig.2 Triangular Surface Mesh & Divided surface near LE and TE

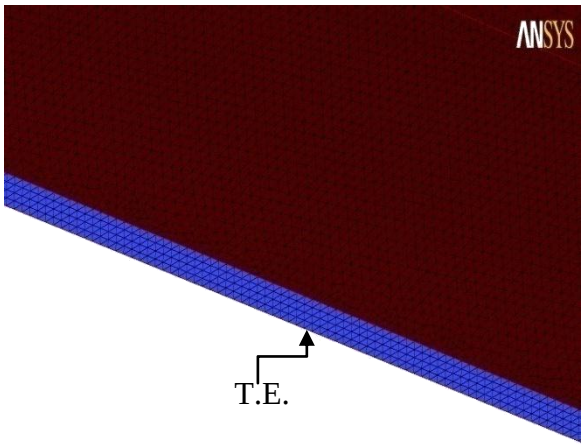

Fig.3 Quadratic elements at Trailing Edge

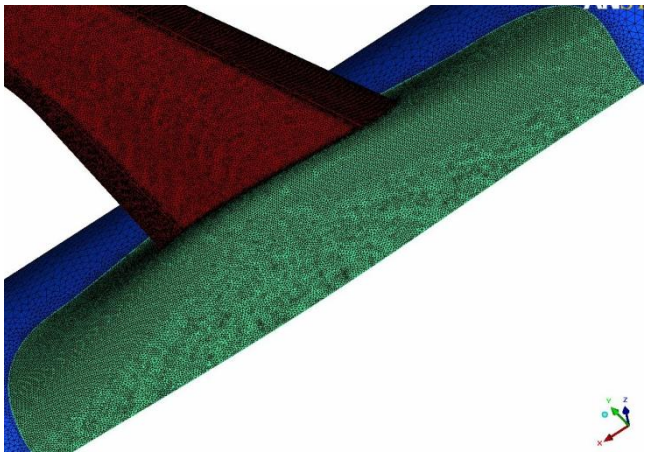

Fig.4 Mesh near wing-fairing-fuselage junction

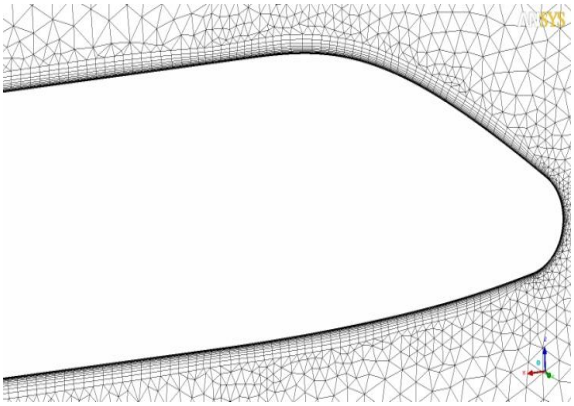

Fig.5 Boundary Layer Mesh (Prism Layers) at symmetry plane

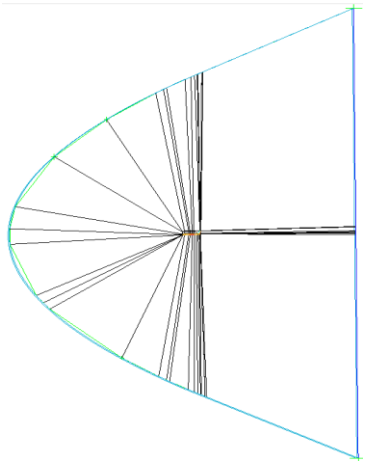

Fig.6 Volume Domain (Parabolic)

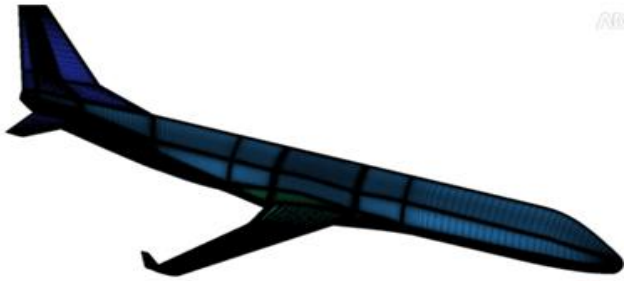

Fig.7 Structured Mesh over Aircraft

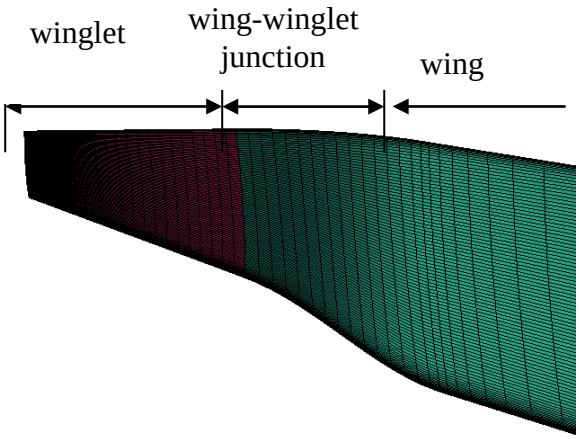

Fig.8 Mesh near wing-winglet junction

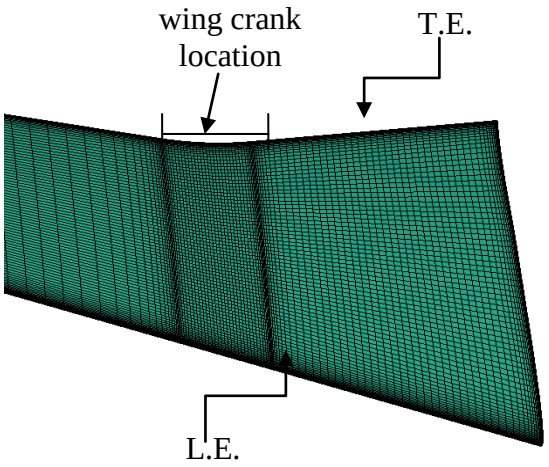

Fig.9 Mesh over cranked region of wing

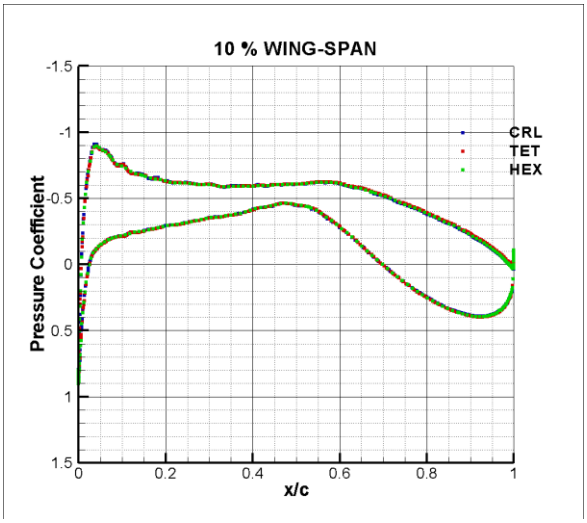

Fig:10 Cp plot 10% span at 0^o AoA

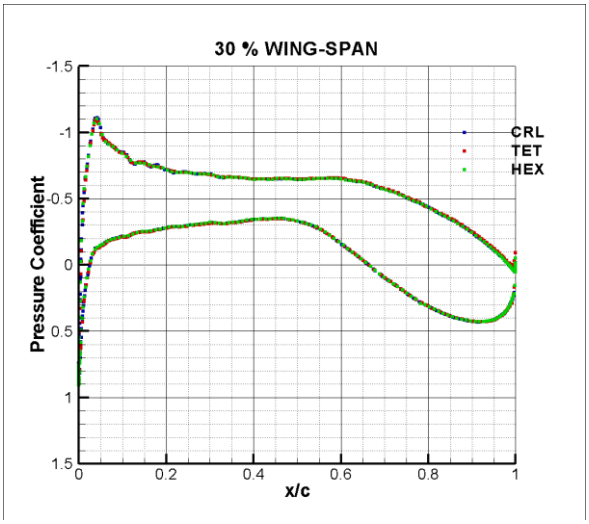

Fig:11 Cp plot 30% span at 0^o AoA

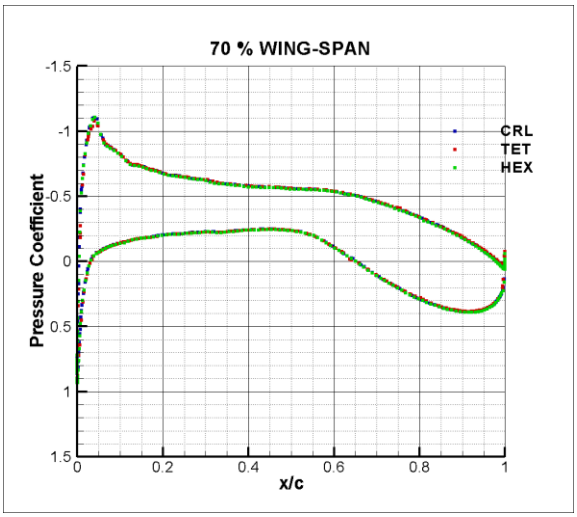

Fig:12 Cp plot 70% span 0° AoA

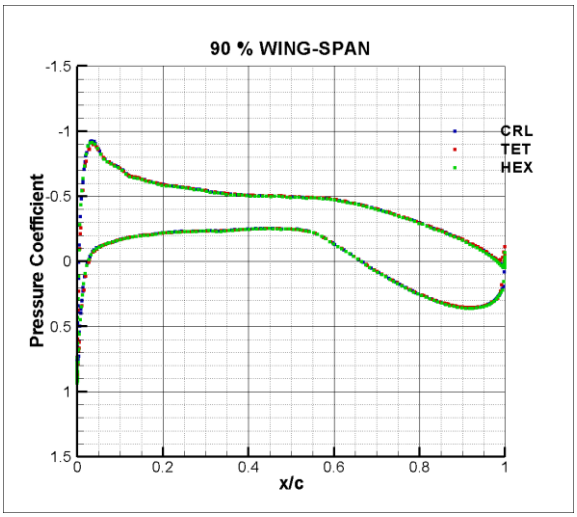

Fig:13 Cp plot 90% span 0° AoA

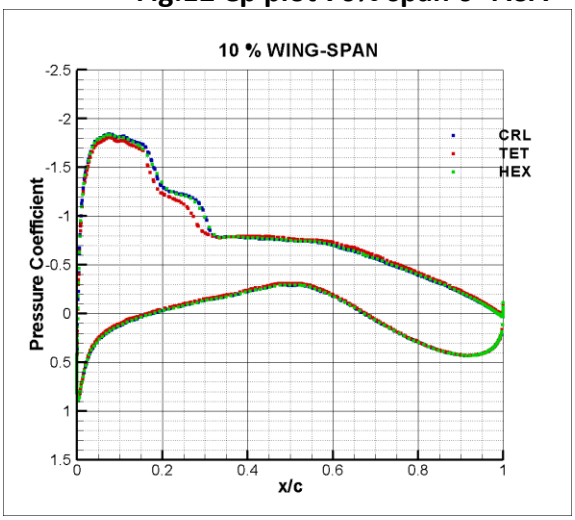

Fig:14 Cp plot 10% span 4° AoA

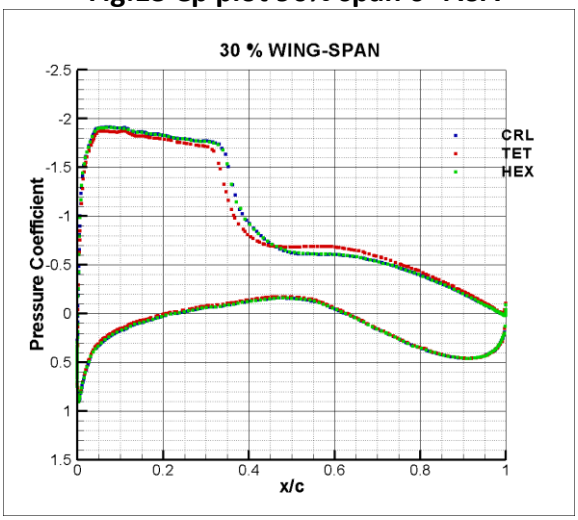

Fig:15 Cp plot 30% span 4° AoA

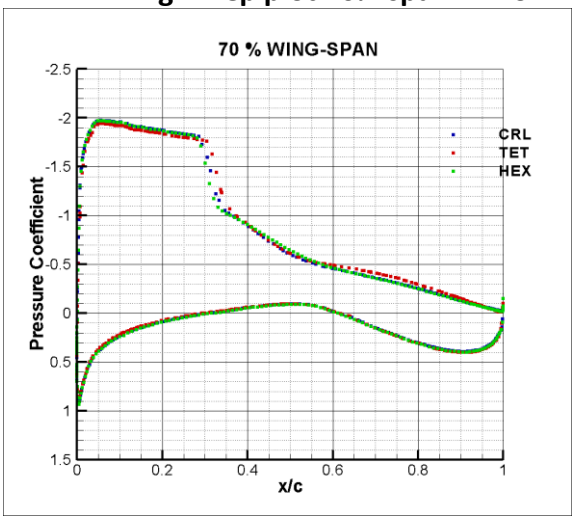

Fig:16 Cp plot 70% span 4° AoA

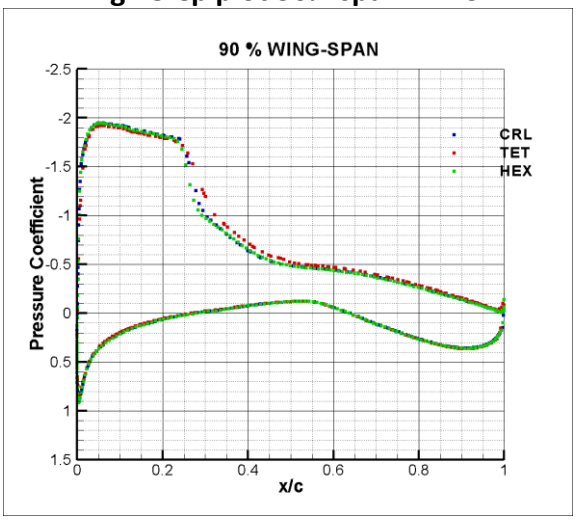

Fig:17 Cp plot 90% span 4° AoA

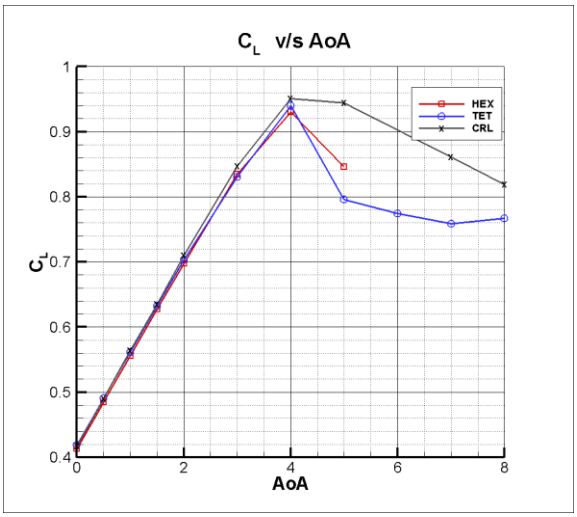

Fig:18 C_L v/s AoA

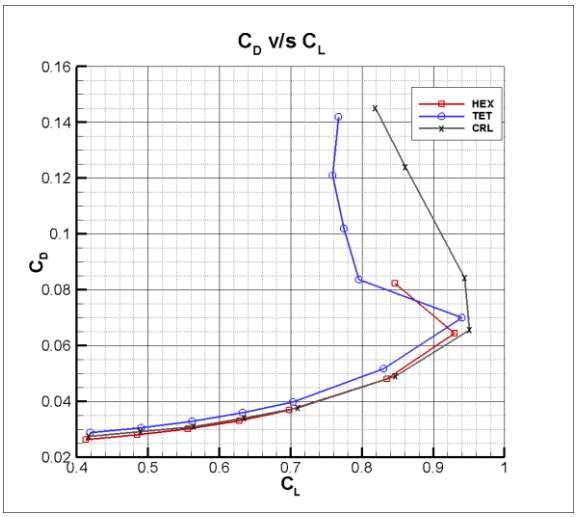

Fig:19 Drag Polar

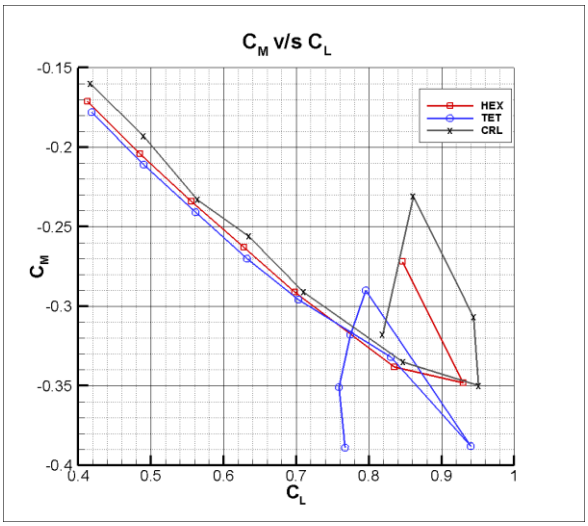

Fig:20 C_M v/s C_L

Scientist, CTFD Division, CSIR-NAL, Post Box No.1779, Bangalore-560017, e-mail: vishalss@nal.res.in